

Light scattering calculations from oleic-acid droplets with water inclusions

D. R. Prabhu

Oracle Corporation, Redwood Shores, CA 94065

Dev.prabhu@oracle.com

Melvin Davies

Clark Atlanta University, Atlanta, Georgia, 30314

Gorden Videen

AMSRL-CI-EM, Army Research Laboratory, 2800 Powder Mill Road, Adelphi, Maryland 20783-1197

gvideen@arl.army.mil

Abstract: We present modeling results in video format showing the changes that occur in the light scattered by a spherical oleic-acid host droplet containing a spherical water inclusion as the inclusion parameters vary. When the system symmetry is broken, a second set of diffraction rings appears on the side opposite the inclusion. The inclusion also acts as a second coherent source, contributing to an interference structure in the scattering pattern, the spatial frequency of which varies with the position of the inclusion.

©2001 Optical Society of America

OCIS codes: (290.0290) Scattering, (290.4210) Multiple scattering, (010.1310) Atmospheric scattering

References and links

1. D. Ngo and R. G. Pinnick, "Suppression of scattering resonances in inhomogeneous microdroplets," *J. Opt. Soc. Am. A* **11**, 1352-1359 (1994).
2. B. V. Bronk, M. J. Smith, and S. Arnold, "Photon-correlation spectroscopy for small spherical inclusions in a micrometer-sized electrostatically levitated droplet," *Opt. Lett.* **18**, 93-95 (1993).
3. H.-B. Lin, A. L. Huston, J. D. Eversole, A. J. Campillo, and P. Chýlek, "Internal scattering effects on microdroplet resonant emission structure," *Opt. Lett.* **17**, 970-972 (1992).
4. J.-G. Xie, T. E. Ruekgauer, R. L. Armstrong, and R. G. Pinnick, "Suppression of stimulated Raman scattering from microdroplets by seeding with nanometer-sized latex particles," *Opt. Lett.* **18**, 340-342 (1993).
5. R. L. Armstrong, J.-G. Xie, T. E. Ruekgauer, and R. G. Pinnick, "Energy-transfer-assisted lasing from microdroplets seeded with fluorescent sol," *Opt. Lett.* **17**, 943-945 (1992).
6. G. Videen, P. Pellegrino, D. Ngo, P. Nachman, and R. G. Pinnick, "Qualitative light-scattering angular correlations of conglomerate particles," *Appl. Opt.* **36**, 3532-3537 (1997).
7. P. Pellegrino, G. Videen, and R. G. Pinnick, "Quantitative light-scattering angular correlations of conglomerate particles," *Appl. Opt.* **36**, 7672-7677 (1997).
8. G. Videen, P. Pellegrino, D. Ngo, J. S. Videen, and R. G. Pinnick, "Light-scattering intensity fluctuations in microdroplets containing inclusions," *Appl. Opt.* **36**, 6115-6118 (1997).
9. U. K. Krieger and C. Braun, "Light-scattering intensity fluctuations in single aerosol particles during deliquescence," *J. Quant. Spectroscopy and Radiative Transfer* (in press).
10. U. K. Krieger and C. Braun, "Light-scattering intensity fluctuations in single aerosol particles during deliquescence," in *Light scattering by nonspherical particles: Halifax contributions*, G. Videen, Q. Fu, P. Chýlek, eds. (Adelphi, US Army Research Laboratory, 2000) 134-137.
11. P. Chýlek and G. Videen, "Scattering by a composite sphere and effective medium approximations," *Opt. Comm.* **146**, 15-20 (1998).
12. D. R. Secker, P. H. Kaye, R. S. Greenaway, E. Hirst, D. Bartley and G. Videen "Light Scattering From Deformed Droplets And Droplets With Inclusions. I: Experimental results," *Appl. Opt.* **39**, 5023-5029 (2000).
13. G. Videen, W. Sun, Q. Fu, D. R. Secker, P. H. Kaye, R. S. Greenaway, E. Hirst, and D. Bartley, "Light Scattering From Deformed Droplets And Droplets With Inclusions. II: Theoretical Treatment," *Appl. Opt.* **39**, 5030-5039 (2000).

14. S. Holler, Yongle Pan, R. K. Chang and J. R. Böttiger, "Two-dimensional angular optical scattering for the characterization of airborne microparticles," *Opt. Lett.* **23**, 18, 1489-1491 (1998).
15. M. D. Barnes, C.-Y. Kung, N. Lerner, K. Fukui, B. G. Sumpter, and D. W. Noid, and J. U. Otaigbe "Homogeneous polymer blend microparticles with a tunable refractive index," *Opt. Lett.* **24**, 121-123 (1999).
16. B. Sachweh, H. Barthel, R. Polke, H. Umhauer and H. Büttner, "Particle shape and structure analysis from the spatial intensity pattern of scattered light using different measuring devices," *J. Aerosol Sci.* **30**, 1257-1270 (1999).
17. S. Holler, J.-C. Auger, B. Stout, Y. Pan, J. R. Böttiger, R. K. Chang and G. Videen, "Observations and Calculations of Light Scattering from Clusters of Spheres," *Appl. Opt.* **39**, 6873-6887 (2000).
18. K. A. Fuller and D. W. Mackowski, "Electromagnetic scattering by compounded spherical particles," in *Light scattering by nonspherical particles: theory, measurements, and applications*, M. I. Mishchenko, J. W. Hovenier, L. D. Travis, eds. (San Diego, Academic Press, 2000) 226-272.
19. See for instance the website maintained by Thomas Wriedt: <http://www.t-matrix.de/>
20. D. Ngo, G. Videen, and P. Chýlek, "A FORTRAN code for the scattering of EM waves by a sphere with a nonconcentric spherical inclusion," *Comp. Phys. Comm.* **1077**, 94-112 (1996).
21. G. Videen, D. Ngo, P. Chýlek, and R. G. Pinnick, "Light scattering from a sphere with an irregular inclusion," *J. Opt. Soc. Am. A* **12**, 922-928 (1995).
22. R. Schuh and T. Wriedt, "T-matrix program and multiple multipole program for light scattering by particles with inclusions," *J. Quant. Spectrosc. Radiat. Transfer* (in press).
23. P. Chýlek, closing address at the Fifth Conference on Electromagnetic and Light Scattering by Non-Spherical Particles, Halifax, August 31, 2000.

1. Introduction

Systems composed of a sphere containing one or more non-concentric spherical inclusions are of interest because they are one of the simplest, non-symmetric systems whose scattering properties can be calculated and that can be produced repeatedly in the laboratory. They also approximate many naturally occurring particle systems; e.g., droplets containing a nucleating particulate. These systems have been the focus of several investigations. Ngo and Pinnick [1] studied the inclusion's effect on the resonance structure of the host particles. Bronk *et al.* [2] studied the statistics of the light scattered by inclusions within the droplets with the goal of characterizing the inclusions. Seeded droplets have also been studied with regard to their fluorescence [3], stimulated Raman scattering [4], and lasing properties [5]. The cross-correlations of the intensity fluctuations measured at two different scattering angles [6,7] as well as the magnitude of the intensity fluctuations [8] were also investigated with the goal of characterizing the inclusions. Krieger and Braun [9,10] examined the intensity fluctuations of aerosol particles during deliquescence. Chýlek and Videen [11] used this system to investigate the accuracy of various effective medium approximations. Secker *et al.* [12] discovered an asymmetry in the light scattered from oleic-acid droplets in humid environments, which was a result of an inclusion that developed inside the droplets at high humidity. This conclusion was verified by imaging the scattering system onto a CCD and by comparing the measured results with calculated results of a host sphere containing an inclusion [13]. This latter research focused on the two-dimensional "spatial" scattering of non-spherical particles, which is the focus of this note.

We are all well aware that the total intensity of the light scattered by a spherical particle is only dependent on the polar angle when the propagation direction of the incident plane wave is assigned the z-axis. Likewise, we know that as soon as the symmetry of the particle system is broken, e.g., by placing an inclusion at some location off the z-axis, that symmetry is lost in the scattering pattern as well; i.e., it cannot be described as a set of concentric rings. It is only recently that inexpensive CCD cameras and efficient codes have made measurements and calculations of the two-dimensional, spatial scattering of a particle system commonplace (see for instance [12-17]). With these developments it is now expected that scattering codes calculate the far field in both θ and ϕ , and that CCD cameras for acquiring the spatial scattering are standard laboratory equipment.

This note is a result of the growing interest in non-spherical particles, specifically particles containing inclusions. The growing body of research in this topic has led to an

increased number of questions, many of which pertain to the actual spatial scattering structure. A recent manuscript [13], showing spatial scattering patterns of an oleic-acid droplet containing a spherical water inclusion, was written in response to experimental work [12]. The spatial scattering shows the familiar, nearly concentric ring structure characteristic of a homogeneous sphere with some distortion. Superimposed on the ring structure is a secondary set of diffraction rings, centered at a point opposite the inclusion, off the specular peak. In addition, in some of the spatial scattering patterns, bands are seen emanating from the center of the scattering pattern in the shape of a V (also seen in Fig. 9 of [12]). In this note, we produce a movie, which shows the development of these scattering structures and their dependence on some of the physical properties of the scattering system, specifically the physical parameters of the inclusion. It is intended to illustrate the rich patterns that result from a perturbation of an otherwise ideal scattering system. It is hoped that viewing the development of the actual scattering patterns as the system parameters are varied will answer some of the questions regarding the features present in the scattering signals.

2. Model

The solution for the light scattered from a sphere containing a non-concentric spherical inclusion is one of the simplest non-symmetric scattering systems to derive. The multi-pole solution can be found by expanding the electric and magnetic fields in terms of vector spherical harmonics about two coordinate systems, each located at the center of one of the spheres. The boundary conditions at each surface interface are satisfied by translating interaction components from one coordinate system to the other coordinate system [18]. The simplicity of the model, coupled with the proliferation of efficient computers and websites providing software distribution [19] has enabled researchers to model the effects of inclusions on droplets. In our simulations we use a modified version of the multiple multi-pole code co-developed by one of the authors [20], which is freely available [19]. The code is based on our derivation [21].

The orientation of the scattering system is shown in Fig. 1. An incident plane wave propagates in the direction of the z -axis and strikes the host sphere centered on the xyz coordinate system. The center of the inclusion sphere is located a distance d from the center of the host sphere and is oriented at angle θ_{inc} from the z -axis. Note that the center of the inclusion sphere is located at a position $(d, \theta_{inc}, 180^\circ)$. This is consistent with θ_{inc} being the incident angle in our previous derivations and programs [20,21]. We have simply performed a coordinate rotation on the T-matrix obtained in this code.

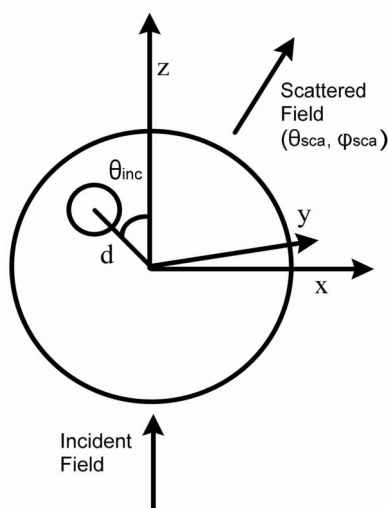


Fig. 1. Orientation of the scattering system is such that the incident plane wave travels in the positive z direction.

As previously noted, convergence problems can occur in this particular code, especially when dealing with large host spheres and when the inclusion is located near the edge of the host [22]. In some situations the problem can be resolved by increasing the number of terms used in the multi-pole (T-matrix) expansions. In some other cases, the convergence problem can be avoided by compiling the program with higher precision variables by default. As with any computational program, it should not be regarded as a black box. One obvious check on the results is that the absorption efficiency is zero when there are no absorbing components present. A great deal of effort has gone into code development in the last decade, and there is no question that more efficient codes exist. The development of other algorithms (like, multiple multi-poles) has enabled researchers to examine the scattering properties of non-spherical inclusions more readily. The computer codes we use have two primary advantages over these techniques: the results can be obtained fairly rapidly for host sizes on the order of a few wavelengths; and the code is readily available. This last factor should not be overlooked. The free distribution of scattering software via the internet has allowed enormous progress to be made in light scattering. It allows almost instant verification of results without costly software development and has led to increased collaborations. As noted previously [23], the maintenance of software libraries and bulletin boards and their contribution to the field should not be overlooked. It is, however, ironic that the maintainer of one of the largest libraries of light-scattering software has not made his codes available on his own library.

3. Results

Figure 2 shows a movie of the spatial light scattering from a spherical oleic-acid host droplet containing a spherical inclusion. The host droplet radius is $R_{\text{host}} = 6\mu\text{m}$, the incident wavelength $\lambda = 0.6328\mu\text{m}$, and the refractive indices of the host and the inclusion are $m_{\text{host}} = 1.4599$, and $m_{\text{inclusion}} = 1.33$. The movie has four views. The upper left shows a graph of the separation distance d between the centers of the inclusion and host, along with the size of the inclusion as a function of the frame number. The upper right shows a graph of the incident angle; i.e., the angular position of the inclusion within the host sphere with respect to the direction of the incident radiation, as a function of the frame number. The lower left shows a cartoon of the scattering system (it should be noted that, although accurate in scale, the orientation of this cartoon is inconsistent with the other graphs; the inclusion should traverse the far side of the host). The arrow shows the direction of the incident radiation. The inclusion moves through the host as the cartoon progresses. Finally, the lower right shows a plot of the total intensity spatial scattering pattern. The radial component of the polar plot is the polar angle θ . The center of the plot is the forward scattering direction ($\theta = 0^\circ$) and the outer circular edge of the plot is the backward scattering direction ($\theta = 180^\circ$). The azimuthal angle ϕ is measured from the horizontal x-axis. The movie begins with a 2-micron-radius inclusion at the center of the host. The inclusion is translated to the forward region of the host sphere (near the hot-spot) at approximately $d = 3\mu\text{m}$. Holding this position d constant, the incident angle is varied until the inclusion is in the backward region of the host. The inclusion then translates to the center. With the incident angle at $\theta_{\text{inc}} = 90^\circ$, the inclusion is translated to the edge of the host ($d = 4\mu\text{m}$), then retreated back to $d = 3\mu\text{m}$, where it shrinks until it disappears ($R_{\text{inclusion}} = 0.0$).

While the inclusion travels along the z-axis, the light scattering total intensity shown in the bottom right of Fig. 2 depends only on the polar angle θ . Since diffraction plays a major role in the forward scatter, we see little change in this region, since diffraction is primarily dependent on the particle morphology rather than its composition. For $\theta > 30^\circ$, there are significant shifts in the positions of the maxima and minima.

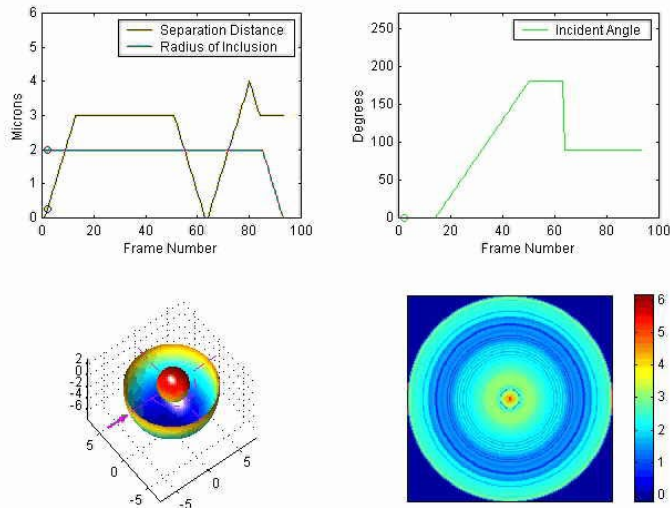


Fig. 2. (1.71 MB) Movie of the light scattered from an oleic-acid droplet containing a water inclusion. Relevant system parameters are shown at the top. Lower left shows a cartoon of the scattering system. Lower right shows the light scattering total intensity.

When the inclusion begins to traverse along the perimeter of the host, the symmetry is broken, and additional structure is present in the scattering patterns. Perhaps the most obvious feature is a second set of diffraction rings located off the z -axis, mentioned in [12,13]. The center of these rings appears on the side opposite the inclusion ($\theta > 0^\circ$, $\phi = 0^\circ$), and their position and brightness is dependent on the incident angle θ_{inc} . They appear to grow out of the center of the pattern as θ_{inc} increases from small values and reach their maximum position and brightness near $\theta_{\text{inc}} = 60^\circ$. As θ_{inc} is further increased, their brightness decreases and they eventually retreat back to the center of the pattern. We note that the number of rings visible increases with inclusion size and their spacing is inversely proportional to the inclusion size. These observations are consistent with the diffraction being a result of the scattering of the internal host fields by the inclusion. Rays striking the host are bent at the surface interface and come to a blurry focus at the hot spot located near the front of the host. It is these rays that are intercepted and scattered by the inclusion. The “specular” direction of this secondary diffraction is in the positive ϕ direction for $\theta_{\text{inc}} > 0$.

The energy of this secondary ring structure is scavenged from the primary ring structure (of the host), which is significantly darker at this location. The inclusion appears to cast a shadow in the primary ring structure. As the inclusion swings around towards the back of the host, the dark, V-shaped bands appear to grow out of this shadow, probably a result of the shadow being distorted as it refracts through the host-surface interface.

One other feature present in the scattering is an interference structure. The inclusion can be thought of as a separate coherent source. Indeed, images of a droplet containing inclusions show them to be sources [2]. The superposition of multiple coherent sources results in an interference pattern, visible in the far-field shown in Fig. 2. This is most apparent when the inclusion traverses the outer perimeter of the host. As θ_{inc} increases, the positions of the fringes appear to emanate from $\phi = 0^\circ$, similar to a moiré pattern produced from two shifting zone plates. The spatial frequency of the fringes appears to increase with the inclusion’s distance from the z -axis. This interference phenomenon is one possible mechanism of the high correlations seen between the measured signals in the forward and backward scatter [6,7]. The measured cross-correlations from a levitated glycerol host droplet containing latex inclusions were seen to switch from highly positive correlations to highly negative correlations with time constants on the order of tenths of seconds. The velocities of the inclusions within the host are very small, but the host is free to rotate within the trap. As the host rotates, the scattered

intensities fluctuate. If the temporal frequencies of the fluctuations are approximately the same at the two scattering angles, then highly positive (or negative) correlations can be measured. As the spatial frequencies change (as they do when the inclusion traverses the perimeter of the host), then the correlations likewise change. Although this is an oversimplified explanation, since the actual systems contained multiple inclusions, it does provide some physical mechanism to explain this phenomenon.

4. Conclusion

The primary purpose of this note is to show the total intensity of the light scattered from a commonly modeled, non-spherical particle system. We have made a number of calculations that demonstrate the rich structure associated with this particle system. Accompanying the primary diffraction pattern of the host droplet is a set of secondary diffraction rings, likely caused by the scattering of the internal fields by the inclusion. The inclusion also appears to cast a shadow on the primary scattering pattern. The inclusion also acts like a source and contributes to an interference structure visible in the scattering. It is hoped that these calculations will shed light on some of the light scattering phenomena seen in these scattering systems.

Acknowledgments

Support for Melvin Davies was provided by the Army Research Laboratory (ARL) Major Shared Resource Center (MSRC) Programming Environment and Training (PET) Summer Institute Program in High Performance Computing (HPC).